

Experimental Ti I oscillator strengths and their application to cool star analysis

R.J. Blackwell–Whitehead^{1*}, H. Lundberg², G. Nave³, J.C. Pickering¹, H.R.A. Jones⁴, Y. Lyubchik⁵, Y.V. Pavlenko⁵, S. Viti⁶

¹*Blackett Laboratory, Imperial College, London, SW7 2BW, UK*

²*Department of Physics, Lund Institute of Technology, P.O.Box 118, 22100 Lund, Sweden*

³*Atomic Physics Division, National Institute of Standards and Technology, 100 Bureau Dr., Gaithersburg, MD 20899, USA*

⁴*Centre for Astrophysics Research, University of Hertfordshire, UK*

⁵*Main Astronomical Observatory, Kiev, Ukraine*

⁶*Department of Physics and Astronomy, University College London, UK*

Accepted for publication 2006 September 26

ABSTRACT

We report experimental oscillator strengths for 88 Ti I transitions covering the wavelength range 465 to 3 892 nm, 67 of which had no previous experimental values. Radiative lifetimes for thirteen energy levels, including the low energy levels $3d^2({}^3F)4s4p({}^3P)z{}^5D_j^o$, have been measured using time resolved laser induced fluorescence. Intensity calibrated Ti I spectra have been measured using Fourier transform spectroscopy to determine branching fractions for the decay channels of these levels. The branching fractions are combined with the radiative lifetimes to yield absolute transition probabilities and oscillator strengths. Our measurements include 50 transitions in the previously unobserved infrared region $\lambda > 1.0 \mu\text{m}$, a region of particular interest to the analysis of cool stars and brown dwarfs.

Key words: atomic data – star: abundances – techniques: spectroscopic

1 INTRODUCTION

Infrared stellar spectroscopy is becoming increasingly important with the advent of better infrared (IR) detectors on ground-based and satellite-borne spectrographs. However, at present the analysis of extensively acquired IR astrophysical spectra is restricted to the study of molecular bands and a small number of atomic transitions in the near IR. A significant restriction on the analysis is the lack of accurate laboratory determined atomic oscillator strengths in the IR. The need for accurate IR atomic oscillator strengths is particularly acute for the study of cool stars and brown dwarfs whose energy distribution peaks in the IR. Accurate oscillator strengths for specific neutral atoms are thus needed to determine fundamental properties, such as effective temperature, metallicity and surface gravity (Lyubchik et al. 2004; Jones et al. 2005a).

The current laboratory atomic database for Ti I is particularly poor in the infrared. The longest wavelength spectral line with a measured oscillator strength is $1.06 \mu\text{m}$ (Whaling et al. 1977). In the wavelength region above $1.06 \mu\text{m}$, the only available oscillator strengths are derived from the semi-empirical calculations of Kurucz (1995). However, theoretical and semi-empirical predictions of oscillator strengths are difficult to calculate to the accuracy required for abundance determinations (uncertainty of 10 to 20 per

cent) especially for weak transitions that may be the only useable lines for the analysis of astrophysical spectra.

The most recent compilation of Ti I oscillator strengths is the work by Martin et al. (1988), which includes the visible to near IR study by Smith & Kühne (1978) and Blackwell et al. (1982a,b, 1983). The Blackwell oscillator strengths were re-examined by Grevesse et al. (1989) who recommended that they be increased by 0.056 dex, or 14 per cent. Since then, Nitz et al. (1998) have published experimentally measured oscillator strengths with uncertainties of about 10 per cent for some even parity levels. Experimental lifetime measurements on Ti I have been carried out by Salih & Lawler (1990); Lawler (1991); Lowe & Hannaford (1991) and Rudolph & Helbig (1982) using time resolved Laser Induced Fluorescence (LIF). Despite the extensive work by Lawler (1991), no experimental lifetimes have been published for the low lying levels, $z{}^5D_j^o$. However, transitions from the $z{}^5D_j^o$ levels are some of the strongest features in the IR Ti I spectrum, and our new measurements have been carried out to obtain accurate laboratory oscillator strengths for these transitions.

The transitions measured in the current work are a selection of strong Ti I lines observed in the near IR that are of importance to the analysis of ultracool dwarf stars, as outlined in Lyubchik et al. (2004). We have measured branching fractions for 88 lines from 465.777 to 3 867.179 nm using high resolution Fourier transform spectroscopy. To place the relative line intensities on an absolute scale, we have measured 13 level lifetimes using time resolved LIF

* E-mail: r.blackwell@imperial.ac.uk (RBW)

and combined these with the branching fractions to yield 88 oscillator strengths, 67 of these being measured for the first time.

2 EXPERIMENTAL MEASUREMENTS

The oscillator strengths have been determined by combining accurate branching fractions with level lifetime measurements. The branching fraction, BF_{ul} , for a transition between upper energy level u and lower energy level l is defined as the ratio of its transition probability, A_{ul} , to the sum of the transition probabilities of all the possible lines from the same upper level:

$$BF_{ul} = \frac{A_{ul}}{\sum_l A_{ul}} = \frac{I_{ul}}{\sum_l I_{ul}} \quad (1)$$

where I_{ul} is the photon intensity of the spectral line. The lifetime, τ_u , of the upper level is the inverse sum of the transition probabilities for all lines from the upper level:

$$\tau_u = \frac{1}{\sum_l A_{ul}} \quad (2)$$

The transition probability for a line is then defined in terms of BF_{ul} and τ_u as:

$$A_{ul} = \frac{BF_{ul}}{\tau_u} \quad (3)$$

We have used the branching fractions and level lifetime technique as outlined above to determine oscillator strengths; the experimental details are described in the following sections.

2.1 Branching fraction measurements

The Ti I spectrum was measured using two spectrometers: the visible to IR (1 800 to 25 000 cm^{-1}) region was recorded at the National Institute of Standards and Technology (NIST) using the NIST 2 m Fourier Transform Spectrometer (FTS) (Nave et al. 1997); and in the visible to UV (15 000 to 30 000 cm^{-1}) at Imperial College (IC) using the IC UV FTS (Pickering 2002). The light source used for both the NIST and IC measurements was a water cooled hollow cathode lamp (HCL) (Danzmann et al. 1988; Learner & Thorne 1988). A pure Ti (99.99 per cent) cathode was used in the HCL, with either Ar or Ne as a buffer gas, to produce a stable source for the Ti I emission spectrum. The optimum running conditions for the Ti HCL were found to be 100 Pa of Ar at a current of 500 mA, and 370 Pa of Ne at a current of 500 mA. To check for self absorption in the main high current measurements, additional low current measurements were recorded with a Ne buffer gas at 200 mA and at a pressure of 345 Pa. Branching fractions were determined using both the spectra recorded with low and high HCL current as discussed by Blackwell-Whitehead et al. (2005). The branching fractions agreed to within the experimental uncertainties, indicating that no self-absorption was present. A summary of the spectra recorded is given in Table 1.

The intensity of the Ti I spectra was calibrated using two tungsten intensity standard lamps; The IC tungsten lamp, calibrated at the National Physical Laboratory (NPL) in the U.K. over the spectral range 12 500 to 33 000 cm^{-1} (800 to 300 nm), has a minimum radiance uncertainty of ± 2.5 per cent (2 standard deviations). The NIST tungsten lamp was calibrated by Optronics Laboratories¹ in

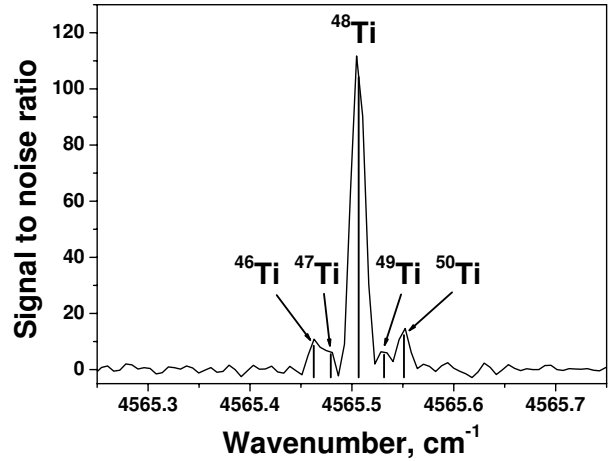


Figure 1. A section of the IR spectrum of Ti I. The $a^5P_2 - z^5D_3^0$ transition at 4565 cm^{-1} exhibits structure due to the five titanium isotopes ^{46}Ti , ^{47}Ti , ^{48}Ti , ^{49}Ti and ^{50}Ti .

the U.S.A., and has a radiance calibration uncertainty of ± 3.0 per cent over the range 1600 to 33000 cm^{-1} (6200 to 300 nm). Spectra of the tungsten lamp were recorded before and after each measurement of the titanium spectrum using the same instrument parameters. Further details of the intensity calibration are discussed by Pickering et al. (2001a).

The most abundant isotope of titanium, ^{48}Ti (73.7 per cent, Rosman & Taylor (1998)), was the major contributor to the Ti I line profiles. In Fig. 1, the individual isotope component lines can be observed. The wavelength, intensity and signal-to-noise ratio of each Ti I line was found by integrating the intensity over the line profile and determining the centre of gravity using computer code XGREMLIN (Nave et al. 1997). The calibrated integrated intensity was used to calculate the branching fractions as described by equation 1.

2.2 Lifetime measurements

The radiative lifetime measurements were carried out at the Lund Laser Centre (LLC) using time resolved LIF. The experiment has been described in detail by Xu et al. (2003), and only a brief description is given here. The experimental apparatus consists of two laser systems, the first of which, a Nd:YAG, laser is used to produce free titanium atoms by laser ablation. The laser radiation has a pulse energy of 2 to 10 mJ and is focused onto a rotating titanium target located in a vacuum chamber that has a residual pressure of about 10^{-4} Pa. The second laser system consists of a seeder injected Nd:YAG laser, a dye laser and a pulse compressor. The Nd:YAG laser in the second system produces pulses of approximately 8 ns in duration, which, after pulse compression, provides a 1 ns pulse. The output pulse is then used to pump a dye laser operating with a DCM dye. The output pulse from the dye laser is tunable in the region 610 to 660 nm and can be frequency-doubled or frequency-tripled as required. The tunable range of the pulse can be extended by focusing the second harmonic or third harmonic of the laser into

¹ Certain trade names and products are mentioned in the text in order to adequately identify the apparatus used to obtain the measurements. In no case

does such identification imply recommendation or endorsement by NIST, IC or the Lund Laser Centre.

Table 1. A summary of the Ti I spectra measured at IC and at NIST.

Spectral range ^a (cm ⁻¹)	Resolution (cm ⁻¹)	Spectrometer	Buffer Gas	Current (mA)	Notes
1 800 – 18 500	0.01	NIST 2m FTS	Ne	500, 200	
1 800 – 18 500	0.01	NIST 2m FTS	Ar	500	
7 500 – 25 000	0.01	NIST 2m FTS	Ar	500	
10 000 – 22 500	0.01	NIST 2m FTS	Ne	500	KG3 filter ^b
15 000 – 30 000	0.03	IC UV FTS	Ne	500	

^a The spectral range is the region over which the spectrum was intensity calibrated.

^b The KG3 filter is a near-IR short-pass filter.

a cell with hydrogen gas at 10⁶ Pa to produce radiation of different stimulated Stokes and anti-Stokes Raman components.

The free titanium atoms produced by laser ablation move across an interaction area where the pulse from the second laser intersects the titanium atoms and induces fluorescence. The two Nd:YAG lasers are externally triggered so that the time between the ablation pulse and the interaction of the excitation pulse with the free atoms can be varied. The LIF is passed through a monochromator in order to allow only one transition from the excited level to be detected. The fluorescence from the $z^5D_j^o$ levels was detected with an IR microchannel plate photomultiplier tube (PMT). All other levels have decay channels in the visible region and hence a visible-region PMT was used. The photomultiplier signal is recorded on an oscilloscope with a real time sampling rate of 2×10^9 samples s⁻¹ and then processed by a computer to determine the decay curve of the LIF signal.

3 RESULTS

3.1 Radiative lifetimes

The radiative lifetime, τ , was determined for each level by fitting exponential decay curves to approximately 20 measurements and taking the average. Of the 13 level lifetimes measured, two have previously published laboratory values (Lawler 1991), providing a comparison with our new measurements in Table 2. The new laboratory lifetime values and the previous values by Lawler (1991) agree to within the experimental uncertainties of both measurements.

For most of our new level lifetimes, the only previously available values for comparison are the semi-empirical calculations of Kurucz (1995). For the $z^5D_j^o$, $z^3F_j^o$ and $z^3D_j^o$ levels, the comparison between experimental lifetimes and the Kurucz (1995) calculations agree to within a few per cent. However, for the higher energy levels the experimental lifetimes are up to a factor of 6 smaller than the theoretical lifetimes.

3.2 Branching fractions and oscillator strengths

Table 3 contains the branching fractions, BF, the transition probabilities, A, and oscillator strengths, log(gf), determined by our measurements. The new oscillator strengths are compared with semi-empirical calculations of Kurucz (1995) and previous experimental data where available. In Table 3, it can be seen that our experimental results and the calculated values for the stronger transitions agree to within ± 50 per cent for the majority of the transitions. The

Ti I wavenumbers, σ , in Table 3 have been calibrated using the accurate Ar II line wavenumbers of Norlén (1973). The wavenumber calibration uncertainty in the Ti I wavenumbers is 0.005 cm⁻¹ and agrees with the values of Forsberg (1991) to within the uncertainties of both measurements.

Since Ti I has a complex energy level structure, transitions from a given upper level can extend from the mid-IR to the UV, but some of these transitions will be too weak to be observed in our experiment. To determine the contribution of weak, unobserved transitions, it is possible to use theoretical predictions to calculate a residual value (the sum of the transition probabilities for all unobserved transitions from a given upper level), e.g. the work on Fe II (Nilsson et al. 2000; Pickering et al. 2001b) and Ti II (Pickering et al. 2001a). For the branching fractions investigated in this paper, the residual values are about 0.1 to 3 per cent and are given at the end of each set of branching fractions in column 5 of Table 3.

The uncertainty of the oscillator strength measurements is determined from the uncertainty in the level lifetimes and the branching fractions. The uncertainty in integrated intensities is determined from the intensity calibration of the observed spectra and the uncertainty in cross-calibrating the line intensities observed in different spectra. The uncertainty in the lifetime measurements is one standard deviation. The uncertainty in the oscillator strength is the sum in quadrature of the uncertainties for both the branching fractions and lifetimes.

It can be seen that our results are consistent with previous experimental measurements for both the weaker and stronger transitions. Of the previous 21 laboratory determined oscillator strengths in Table 3, 16 agree to within the experimental uncertainties of both measurements. Although most of our measurements agree well with the oscillator strengths of Blackwell et al. (1983) that have been revised by Grevesse et al. (1989), the four IR transitions from the $z^3D_j^o$ levels measured by Blackwell et al. (1983) are 56 per cent (0.25 dex) weaker than our measurements. This may be the result of non-thermal equilibrium effects in the King furnace technique used by Blackwell et al. (1983) or an inaccuracy in the measured furnace temperature for the near IR oscillator strengths. It was noted by Blackwell et al. (1983) that these 4 lines gave a solar titanium abundance that was 0.15 dex (40 per cent) higher than the lines at shorter wavelengths, and they attributed this to blends in the solar spectrum. Although their values agreed well with Kurucz & Peytremann (1975), the more recent calculations of Kurucz (1995) show much better agreement with our data than those of Blackwell et al. (1983). Our oscillator strengths for the transitions from the $z^3D_j^o$ levels agree with the calculations of Kurucz (1995) and to within uncertainties of the experimen-

Table 2. Radiative lifetime measurements of Ti I levels.

Configuration	Term	J	Energy (cm ⁻¹) ^a	Lifetime, τ (ns)		
				This work ^b	Previous ^c	Theory ^d
3d ² (³ F)4s4p(³ P)	<i>z</i> ⁵ D ^o	1	18 482.772	500(50)		532
	<i>z</i> ⁵ D ^o	2	18 525.059	530(50)		529
	<i>z</i> ⁵ D ^o	3	18 593.946	550(50)		526
	<i>z</i> ⁵ D ^o	4	18 695.133	520(50)		529
3d ² (³ F)4s4p(³ P)	<i>z</i> ³ F ^o	2	19 322.984		202(10)	218
	<i>z</i> ³ F ^o	3	19 421.580	205(10)	204(10)	220
	<i>z</i> ³ F ^o	4	19 573.973	210(10)	208(10)	224
3d ² (³ F)4s4p(³ P)	<i>z</i> ³ D ^o	1	19 957.852		167(8)	160
	<i>z</i> ³ D ^o	2	20 006.042		180(9)	173
	<i>z</i> ³ D ^o	3	20 126.060		190(10)	188
3d ² (³ F)4s4p(³ P)	<i>z</i> ³ G ^o	3	21 469.487		362(18)	602
	<i>z</i> ³ G ^o	4	21 588.494		336(17)	524
	<i>z</i> ³ G ^o	5	21 739.707		319(16)	472
3d ² 4s(⁴ F)5p	<i>r</i> ³ F ^o	2	43 467.537	14.0(1.0)		22
	<i>r</i> ³ F ^o	3	43 583.354	14.7(1.0)		22
	<i>r</i> ³ F ^o	4	43 744.793	13.7(1.0)		23
3d ² 4s(⁴ F)5p	³ G ^o	3	44 155.594	15.9(1.0)		68
	³ G ^o	4	44 257.097	15.8(1.0)		68
	³ G ^o	5	44 375.501	4.2(0.3)		26
3d ³ (² F)4p	<i>s</i> ³ G ^o	4	46 837.983	44(4)		8

^a Energy level values taken from Forsberg (1991)

^b Uncertainty in parenthesis (nm) is one standard deviation.

^c Previous laboratory measurements by Lawler (1991)

^d Semi-empirical values calculated by Kurucz (1995)

tal measurements of Smith & Kühne (1978) and Blackwell et al. (1982a). Therefore we believe that the near IR oscillator strengths of Blackwell et al. (1983) should be reduced by 0.25 dex.

3.3 Comparison with cool star spectra

The new Ti I oscillator strengths presented in Table 3 include transitions listed by Lyubchik et al. (2004) as important for the analysis of ultra cool dwarf stars. In total, five of the new oscillator strengths are listed by Lyubchik et al. (2004) as first priority transitions, thirteen are listed as second priority and three as third priority. In Fig. 2, we show an observed spectrum of the M2 dwarf GJ806. The spectrum was acquired by Doppmann et al. (2005) using the *NIR-SPEC* instrument on the Keck Telescope and has a resolution of 17000. The theoretical spectrum was generated by the WITA6 programme (Pavlenko 2000), and used the NEXTGEN model structures supplied by Hauschildt et al. (1999). The theoretical spectrum was computed with a wavelength step of 0.001 nm and convolved with a Gaussian to match the instrumental broadening. The Ti I lines identified in Fig. 2 have also been measured in the laboratory to determine accurate oscillator strengths, see Table 3. The experimental values are the first laboratory determined oscillator strengths for these transitions, which are all identified as priority 1 lines by Lyubchik et al. (2004). This prioritization is an indication that they are amongst the relatively few identifiable atomic lines

that are predicted to be observable and suitable for the high precision analysis of cool stars and brown dwarfs. Whilst the Ti I lines are clearly the strongest features in the observed spectrum and are reasonably well fitted in Fig. 2, it can also be seen that the continuum is rather poorly described. A better fit of the continuum would benefit from a line-by-line identification of the species responsible. In particular, scrutiny should be made of the large numbers of molecular water vapour lines expected to be present in this region as indicated by Jones et al. (2005b). A detailed analysis of this observational spectrum, and others that we are acquiring in wavelength regions containing Ti I lines with experimentally determined oscillator strengths, will be the subject of a further paper (Lyubchik et al., in preparation).

4 SUMMARY

Experimental oscillator strengths have been determined for 88 lines of Ti I in the visible and IR regions of the spectrum. Sixty six of these transitions have no previous experimental oscillator strengths. The uncertainty in the oscillator strengths is 10 to 15 per cent for the stronger transitions, and for all oscillator strengths in Table 3 the uncertainty has been reduced to < 25 per cent.

In the IR region $\lambda > 1.0 \mu\text{m}$, 50 new oscillator strengths have been measured, including those identified as high priority by

Table 3. Experimental and semi-empirical transition probabilities for Ti I

Upper level	Lower level	Transition λ_{vac} (nm)	σ (cm ⁻¹) ^b	BF	BF Unc. (per cent)	A ^a (10 ⁷ s ⁻¹)	This work log(gf)	Unc. ^c	Previous Experiment log(gf)	Unc. ^c	Ref. ^d	Expt – Theory (per cent) ^e
z ⁵ D ₁ ^o	a ⁵ F ₁	838.5085	11925.938	0.306	5	6.11	-1.71	0.04				8
	a ⁵ F ₂	841.4670	11884.008	0.641	5	12.82	-1.39	0.04				8
	a ⁵ P ₁	2221.7299	4500.997	0.037	5	0.75	-1.78	0.04				13
	a ⁵ P ₂	2245.0052	4454.333	0.010	6	0.19	-2.36	0.05				-13
		Residual			0.006							
z ⁵ D ₂ ^o	a ⁵ F ₁	835.5458	11968.225	0.024	8	0.46	-2.62	0.05	-2.62	0.06	(4)	-5
	a ⁵ F ₂	838.4834	11926.294	0.258	5	4.86	-1.59	0.04				0
	a ⁵ F ₃	842.8822	11864.054	0.635	5	11.97	-1.20	0.04	-1.19	0.05	(3)	-3
	a ⁵ P ₁	2201.0514	4543.283	0.018	5	0.34	-1.91	0.04				5
	a ⁵ P ₂	2223.8927	4496.620	0.029	5	0.56	-1.69	0.04				5
	a ⁵ P ₃	2262.7392	4419.422	0.003	12	0.05	-2.74	0.06				-20
		Residual			0.033							
z ⁵ D ₃ ^o	a ⁵ F ₂	833.6681	11995.181	0.018	5	0.32	-2.63	0.04				-5
	a ⁵ F ₃	838.0164	11932.941	0.191	5	3.48	-1.59	0.04				-5
	a ⁵ F ₄	843.7971	11851.190	0.707	5	12.85	-1.02	0.04				-5
	a ³ P ₂	1000.8408	9991.600	0.001	19	0.02	-3.65	0.08				-38
	a ⁵ P ₂	2190.3367	4565.508	0.037	5	0.68	-1.47	0.04				10
	a ⁵ P ₃	2228.0101	4488.310	0.017	5	0.31	-1.80	0.04				3
	Residual			0.029								
z ⁵ D ₄ ^o	a ⁵ F ₃	830.9705	12034.122	0.006	7	0.12	-2.97	0.05				-15
	a ⁵ F ₄	836.6539	11952.374	0.108	5	2.07	-1.71	0.04				3
	a ⁵ F ₅	843.7278	11852.163	0.807	5	15.52	-0.83	0.04				3
	a ⁵ P ₂	2178.8892	4589.495	0.056	4	1.07	-1.17	0.04				13
		Residual			0.024							
z ³ F ₂ ^o	a ³ F ₂	517.5183	19322.987	0.855	10	42.34	-1.07	0.04	-1.06	0.05	(2)	5
	a ³ F ₃	522.1155	19152.852	0.055	13	2.71	-2.26	0.06	-2.23	0.05	(2)	3
	b ³ F ₂	1283.4950	7791.226	0.066	10	3.26	-1.40	0.04				33
	b ³ F ₃	1301.5452	7683.176	0.011	10	0.52	-2.18	0.04				40
	a ³ G ₃	2372.5504	4214.874	0.012	10	0.59	-1.61	0.04				60
		Residual			0.002							
z ³ F ₃ ^o	a ³ F ₂	514.8912	19421.577	0.094	10	4.58	-1.89	0.05	-1.95	0.05	(2)	18
	a ³ F ₃	519.4416	19251.443	0.787	10	38.60	-0.96	0.04	-0.95	0.05	(2)	5
	a ³ F ₄	525.3563	19034.700	0.016	21	0.81	-2.63	0.08	-2.39	0.05	(2)	-53
	a ⁵ F ₄	788.7169	12678.821	0.003	14	0.14	-3.05	0.06				45
	b ³ F ₂	1267.4562	7889.819	0.007	10	0.33	-2.25	0.04				33
	b ³ F ₃	1285.0552	7781.767	0.067	10	3.29	-1.25	0.04				43
	b ³ F ₄	1308.0847	7644.765	0.009	10	0.46	-2.08	0.04				45
	a ³ G ₃	2318.3240	4313.461	0.001	14	0.04	-2.70	0.06				43
	a ³ G ₄	2344.7878	4264.778	0.012	10	0.60	-1.46	0.04				70
		Residual			0.004							
z ³ F ₄ ^o	a ³ F ₃	515.3619	19403.839	0.073	8	3.51	-1.90	0.04	-1.96	0.05	(2)	15
	a ³ F ₄	521.1836	19187.098	0.808	6	38.85	-0.85	0.04	-0.82	0.05	(2)	3
	a ⁵ F ₅	785.4838	12731.008	0.006	8	0.28	-2.64	0.04				50
	b ³ F ₃	1260.3724	7934.163	0.007	6	0.33	-2.15	0.04				50
	b ³ F ₄	1282.5179	7797.162	0.088	6	4.22	-1.03	0.04				55
	a ¹ G ₄	1341.2775	7455.579	0.001	10	0.05	-2.95	0.05				-55
	a ³ G ₄	2263.8914	4417.173	0.001	10	0.04	-2.56	0.04				75
	a ³ G ₅	2296.9602	4353.580	0.016	6	0.76	-1.27	0.04				88
		Residual			0.001							

^a Transition probability

^b Wavenumber as observed in Fourier transform spectra.

^c The uncertainty in log(gf) expressed in dex, where ± 0.01 dex corresponds to approximately ± 2.5 per cent.

^d References: (1) Smith & Kühne (1978); (2) Blackwell et al. (1982a); (3) Blackwell et al. (1982b); (4) Blackwell et al. (1983).

^e Percentage difference between our new log(gf) values and the calculated values of Kurucz (1995).

Table 3 – *continued* Experimental and semi-empirical transition probabilities for Ti I

Upper level	Lower level	Transition		BF	BF Unc. (per cent)	A ^a (10 ⁷ s ⁻¹)	This work		Previous Experiment			Expt – Theory (per cent) ^e	
		λ_{vac} (nm)	σ (cm ⁻¹) ^b				log(gf)	Unc. ^c	log(gf)	Unc. ^c	Ref. ^d		
z ³ D ₁ ^o	a ³ F ₂	501.5585	19937.853	0.848	9	50.79	-1.24	0.04	-1.22	0.10	(1)	-8	
	a ³ P ₀	869.4719	11501.235	0.050	9	2.99	-1.99	0.04	-2.24	0.06	(4)	18	
	a ³ P ₁	873.7112	11445.429	0.038	9	2.30	-2.10	0.04	-2.33	0.06	(4)	20	
	b ³ F ₂	1189.6135	8406.092	0.059	9	3.52	-1.65	0.04				23	
	a ³ D ₁	3893.5967	2568.319	0.001	15	0.07	-2.33	0.06				2	
		Residual			0.004								
z ³ D ₂ ^o	a ³ F ₂	499.8490	20006.042	0.083	10	4.59	-2.07	0.04	-2.06	0.05	(2)	-15	
	a ³ F ₃	504.1363	19835.908	0.766	9	42.56	-1.09	0.04	-1.07	0.06	(4)	-5	
	a ⁵ F ₂	745.8638	13407.273	0.002	16	0.08	-3.46	0.07				8	
	a ⁵ F ₃	749.3424	13345.034	0.001	20	0.07	-3.56	0.08				5	
	a ¹ D ₂	784.2716	12750.686	0.002	16	0.11	-3.28	0.07				3	
	a ³ P ₁	868.5367	11513.619	0.065	9	3.59	-1.69	0.04	-1.88	0.06	(4)	8	
	a ³ P ₂	876.9086	11403.697	0.022	9	1.20	-2.16	0.04				7	
	b ³ F ₂	1180.0409	8474.283	0.010	9	0.54	-2.25	0.04				18	
	b ³ F ₃	1195.2815	8366.230	0.047	9	2.63	-1.55	0.04				10	
	a ³ D ₂	3872.6956	2582.181	0.001	11	0.08	-2.07	0.05				25	
		Residual			0.002								
z ³ D ₃ ^o	a ³ F ₃	501.1042	19955.929	0.043	13	2.24	-2.23	0.06	-2.20	0.05	(2)	-25	
	a ³ F ₄	506.6065	19739.185	0.788	9	41.49	-0.95	0.04	-0.94	0.05	(2)	-3	
	a ⁵ F ₄	747.2000	13383.297	0.002	12	0.12	-3.15	0.05				35	
	a ¹ D ₂	776.9583	12870.704	0.003	13	0.14	-3.06	0.06				18	
	a ³ P ₂	867.7757	11523.715	0.088	9	4.61	-1.44	0.04	-1.61	0.06	(4)	3	
	b ³ F ₃	1178.3772	8486.247	0.009	9	0.45	-2.18	0.04				13	
	b ³ F ₄	1197.7131	8349.245	0.051	9	2.69	-1.39	0.04				13	
	a ³ D ₃	3867.1786	2585.865	0.001	10	0.08	-1.93	0.04				10	
		Residual			0.016								
z ³ G ₃ ^o	a ³ F ₂	465.7772	21469.493	0.810	11	22.38	-1.29	0.05	-1.28	0.05	(2)	60	
	b ³ F ₂	1006.2662	9937.728	0.028	11	0.78	-2.08	0.05				30	
	b ³ F ₃	1017.3276	9829.676	0.002	16	0.06	-3.17	0.07				5	
	a ¹ G ₄	1069.3930	9351.100	0.002	18	0.05	-3.22	0.08				-70	
	a ³ G ₃	1571.9872	6361.375	0.088	10	2.43	-1.20	0.05				23	
	a ³ G ₄	1584.1108	6312.690	0.011	11	0.29	-2.12	0.05				28	
	a ³ D ₂	2472.0023	4045.304	0.001	23	0.01	-3.05	0.09				500	
	a ³ H ₄	2913.5219	3432.272	0.028	10	0.76	-1.17	0.05				28	
	b ¹ G ₄	3142.7448	3181.932	0.003	11	0.09	-2.03	0.05				353	
		Residual			0.028								
	z ³ G ₄ ^o	a ³ F ₃	466.8891	21418.362	0.818	10	24.33	-1.15	0.05	-1.13	0.05	(2)	50
b ³ F ₃		1005.1583	9948.682	0.029	10	0.86	-1.93	0.04				30	
b ³ F ₄		1019.1939	9811.676	0.002	15	0.06	-3.10	0.06				15	
a ³ G ₃		1543.1200	6480.377	0.004	11	0.13	-2.38	0.05				18	
a ³ G ₄		1554.8008	6431.692	0.086	10	2.55	-1.08	0.04				30	
a ³ G ₅		1570.3276	6368.098	0.010	11	0.29	-2.01	0.05				40	
a ³ H ₄		2815.8907	3551.274	0.001	13	0.03	-2.53	0.06				-7	
a ³ H ₅		2900.8846	3447.224	0.029	10	0.86	-1.01	0.04				45	
		Residual			0.022								
z ³ G ₅ ^o	a ³ F ₄	468.3220	21352.832	0.832	10	26.09	-1.03	0.04	-1.01	0.05	(2)	43	
	b ³ F ₄	1003.7242	9962.896	0.033	10	1.03	-1.77	0.04				38	
	a ³ G ₄	1519.0857	6582.907	0.004	11	0.13	-2.32	0.05				33	
	a ³ G ₅	1533.9037	6519.314	0.091	10	2.84	-0.96	0.04				28	
	a ³ H ₅	2778.9797	3598.443	0.001	12	0.03	-2.40	0.05				10	
	a ³ H ₆	2819.1750	3547.137	0.034	10	1.07	-0.85	0.04				58	
		Residual			0.006								

^a Transition probability^b Wavenumber as observed in Fourier transform spectra.^c The uncertainty in log(gf) expressed in dex, where ± 0.01 dex corresponds to approximately ± 2.5 per cent.^d References: (1) Smith & Kühne (1978); (2) Blackwell et al. (1982a); (3) Blackwell et al. (1982b); (4) Blackwell et al. (1985).^e Percentage difference between our new log(gf) values and the calculated values of Kurucz (1995).

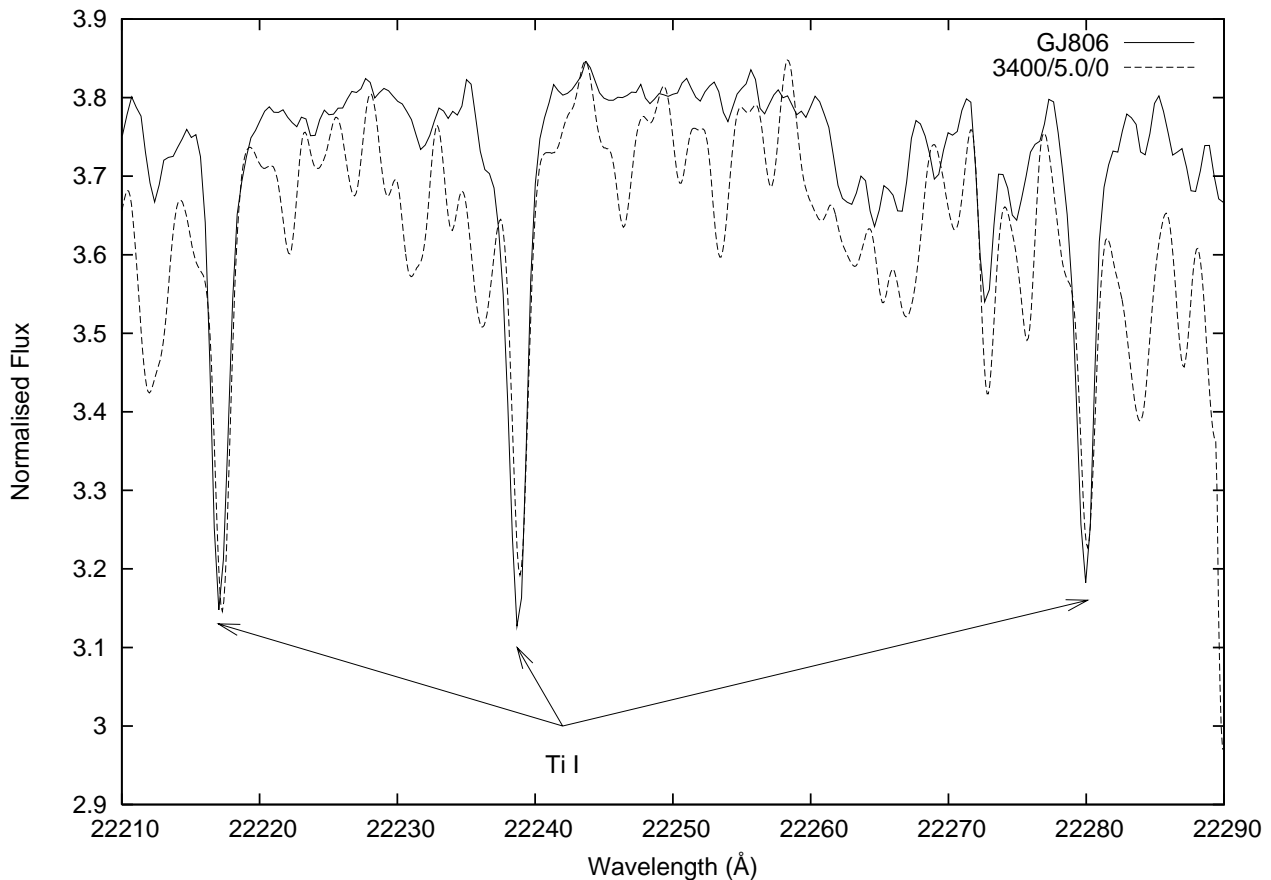


Figure 2. A section of an observed infrared spectrum from the cool dwarf star GJ806 is compared with a 3 400 K, solar metallicity, $\log(g) = 5.0$ theoretical spectrum (3400/5.0/0) using the new water line list from Barber et al. (2006), and computed from the model structure provided by Hauschildt et al. (1999). The three labelled Ti I lines are all ones whose measured oscillator strengths have been described for the first time in this paper. They are all denoted as high priority lines for the precision study of cool stars by Lyubchik et al. (2004).

Lyubchik et al. (2004). We show that some of these features are readily identifiable in cool star spectra and are likely to be of substantial interest for measurement of effective temperatures, gravities and metallicities. It can be seen that oscillator strengths for transitions in the infrared region $\lambda > 1.0 \mu\text{m}$ show a marked deviation from the semi-empirical calculations of Kurucz (1995), which were the only available data for these lines prior to our work. Whilst theoretical calculations provide important data in regions of the spectrum where experimental data are not available, it is important to note that significant differences between theoretical calculations and experimental measurements do occur. In particular, for weaker transitions, caution should be exercised when relying solely on theoretical calculations for oscillator strengths. This is of particular importance for the analysis of cool stars and brown dwarfs where visible transitions are too weak to be of diagnostic value and oscillator strengths in the IR are required.

ACKNOWLEDGMENTS

RBW and JCP gratefully acknowledge the financial support of PPARC of the UK and the Leverhulme Trust. GN acknowledges the financial support of the National Aeronautical and Space Administration under inter-agency agreement W-10,255. HL acknowledges the support of the EU-TMR access to Large-Scale Facility Pro-

gramme (contract RII3-CT-2003-506350). We are also very grateful to Kevin Covey for making the spectrum of GJ806 available to us.

REFERENCES

- Barber R.J., Tennyson J., Harris G.J., Tolchenov R., 2006, MNRAS, 368, 107
- Blackwell D.E., Menon S.L.R., Petford A.D., 1983, MNRAS, 204, 883
- Blackwell D.E., Petford A.D., Shallis M.J., Legget S., 1982a, MNRAS, 199, 21
- Blackwell D.E., Petford A.D., Shallis M.J., 1982b, MNRAS, 201, 611
- Blackwell-Whitehead R.J., Xu H.L., Pickering J.C., Nave G., Lundberg H., 2005, MNRAS, 361, 1281
- Danzmann K., Günther M., Fischer J., Kock M., Kühne M., 1988, Appl. Opt., 27, 4947
- Doppmann G.W., Greene T.P., Covey K.R., Lada C.J., 2005, AJ, 130, 1145
- Forsberg P., 1991, Phys. Scr., 44, 446
- Grevesse N., Blackwell D.E., Petford A.D., 1989, A&A, 208, 157
- Hauschildt P.H., Allard F., Baron E., 1999, ApJ, 512, 377
- Jones H.R.A., Viti S., Tennyson J., Barber B., Harris G., Pick-

- ering J.C., Blackwell-Whitehead R., Champion J.-P., Allard F., Hauschildt P. H., Jorgensen U. G., Ehrenfreund P., Stachowska E., Ludwig H.-G., Martín E. L., Pavlenko Ya., Lyubchik Yu., Kurucz R. L., 2005, *Astronomische Nachrichten*, 326, 920
- Jones H.R.A., Pavlenko Ya., Viti S., Barber R.J., Yakovina L., Pinfield D. Tennyson J., 2005, *MNRAS*, 358, 105
- Kurucz R.L., Peytreman, E.A., 1975, "A Table of Semiempirical gf Values" (in three parts), Smithsonian Astrophysical Observatory Special Report 362.
- Kurucz R.L., 1995, *Atomic Data for Ti I*, Kurucz CD-ROM No. 20 Cambridge, Mass.: Smithsonian Astrophysical Observatory
- Lawler J.E., 1991, *A&A*, 252, 853
- Learner R.C.M., Thorne A.P., 1988, *J. Opt. Soc. Am. B*, 5, 2045
- Lowe R.M., Hannaford P., 1991, *Z. Phys. D*, 21, 205
- Lyubchik Y., Jones H.R.A., Pavlenko Y.V., Viti S., Pickering J.C., Blackwell-Whitehead R., 2004, *A&A*, 416, 655
- Martin G.A., Fuhr J.R., Wiese W.L., 1988, *J. Phys. Chem. Ref. Data*, 17, Suppl. 3, 415
- Nave G., Sansonetti C.J., Griesmann U., 1997, in *Opt. Soc. Am. Tech. Digest Series*, 3, *Fourier transform spectroscopy: Methods and Applications* (Washington DC:Opt. Soc. Am.), 38
- Nilsson H., Sikström C.M., Li Z.S., Lundberg H., Raassen A.J.J., Johansson S., Leckrone D.S., Svanberg S., 2000, *A&A*, 362, 410
- Nitz D.E., Wickliffe M.E., Lawler J.E., 1998, *ApJS*, 117, 313
- Norlén, G., 1973, *Phys. Scr.*, 8, 249
- Pavlenko Ya.V., 2000, *Astron. Rept.*, 44, 219
- Pickering J.C., 2002, *Vib. Spectrosc.*, 29, 27
- Pickering J.C., Johansson S, Smith P.L., 2001b, *A&A*, 377, 361
- Pickering J.C., Thorne A.P., Perez R., 2001a, *ApJS*, 132, 403
- Rosman K.J.R., Taylor P.D.P., 1998, *Pure & Appl. Chem.*, 70, 217
- Rudolph J., Helbig V., 1982, *J. Phys. B*, 15, L599
- Salih S., Lawler J.E., 1990, *A&A*, 239, 407
- Smith P. L., Kühne M., 1978, *Proc. R. Soc. London, Ser. A* 362, 263
- Whaling W., Scalo J.M., Testerman L., 1977, *ApJ*, 212, 581
- Xu H.L., Svanberg P., Quinet H.P., Biémont E., 2003, *J. Phys. B*, 36, 4773

This paper has been typeset from a $\text{\TeX}/\text{\LaTeX}$ file prepared by the author.